

Strategies toward phosphorus-containing PAHs and the effect of P-substitution on the electronic properties

Rózsa Szűcs, François Riobé, Aude Escande, Damien Joly, Pierre-Antoine Bouit, László Nyulászi, Muriel Hissler

▶ **To cite this version:**

Rózsa Szűcs, François Riobé, Aude Escande, Damien Joly, Pierre-Antoine Bouit, et al.. Strategies toward phosphorus-containing PAHs and the effect of P-substitution on the electronic properties. Pure and Applied Chemistry, 2017, 88 (3), pp.341-356. 10.1515/pac-2016-0909 . hal-01450088

HAL Id: hal-01450088

https://univ-rennes.hal.science/hal-01450088

Submitted on 2 Feb 2017

HAL is a multi-disciplinary open access archive for the deposit and dissemination of scientific research documents, whether they are published or not. The documents may come from teaching and research institutions in France or abroad, or from public or private research centers.

L'archive ouverte pluridisciplinaire **HAL**, est destinée au dépôt et à la diffusion de documents scientifiques de niveau recherche, publiés ou non, émanant des établissements d'enseignement et de recherche français ou étrangers, des laboratoires publics ou privés.

Rózsa Szűcs, François Riobé, Aude Escande, Damien Joly, Pierre-Antoine Bouit, László Nyulászi,* Muriel Hissler*

Strategies toward phosphorus-containing PAHs and the effect of P-substitution on the electronic properties

In this paper, we report on the different synthetic strategies which led to the preparation of a whole family of polyaromatic hydrocarbons containing a P-atom at the edge. In particular, we show from both experimental and theoretical perspective how the Scholl method has to be adapted to the specificity of organophosphorus derivatives. The P-modified PAHs possess the classical phosphane reactivity that allows fine-tuning of their electronic properties as evidenced by spectro-electrochemistry and theoretical calculations. In particular, the effect of P-substitution on the aromaticity of the different cycles of the PAH was studied.

Keywords : Polyaromatics ; Organophosphorus chemistry; Spectro-electrochemistry; Aromaticity

Introduction

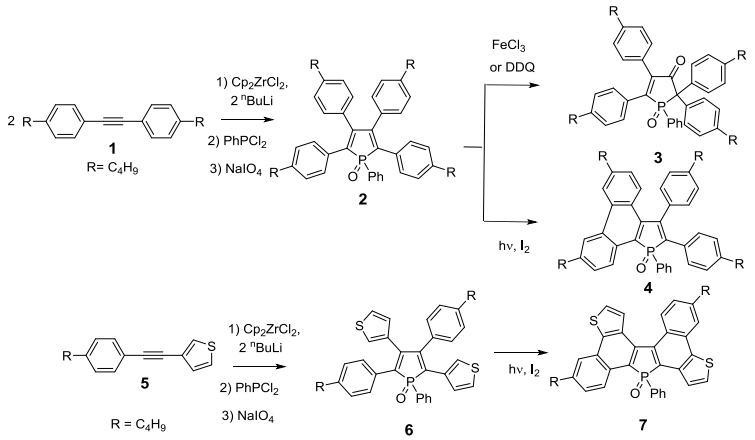
Polycyclic aromatic hydrocarbons (PAHs) have attracted considerable attention, since these 2-dimensional π-conjugated systems[1,2] hold promise for applications in the emerging areas of molecular electronics and optoelectronic devices such as field-effect transistors or organic solar cells.[3] Introduction of heteroatoms into these 2D C-sp^2 platforms appeared recently as an original way to tune their electronic properties.[4,5,6,7,8] Effectively, the nature of the heteroatom and its specific reactivity strongly impact the properties of the doped-PAHs. Furthermore, the physical properties and π-stacking behavior of the doped-PAHs is also effectively influenced by the position (periphery or central) of the heteroatom in the polycyclic scaffold. For example, Clark and co-workers[9] showed by theoretical calculations that centrally positioned P- (and CH-) doping destroys the continuous π-system in the PAHs due to the apparent phosphorus pyramidalization.[10] In contrast, doping with boron or nitrogen in this position retains the planarity of the system while exerting a significant impact on the π-conjugation. These theoretical studies are in accordance with the synthesis of a

curved triarylphosphane presenting a nonplanar structure due to the presence of the pyramidal P-atom within its π-framework.[11] In contrast, the insertion of the σ^3,λ^3-P at the edge of a PAH may lead to planar C-sp^2-structures, and subsequent phosphorus chemistry can be used for molecular engineering of the organic π-materials. The molecular engineering of PAHs based on the reactivity of the heteroatom is only possible when having efficient synthetic ways toward these compounds. The Scholl reaction (cyclodehydrogenation) is by far the most widely used method for the "graphenization" of PAHs.[12,13] For instance, Müllen *et al.* applied the Scholl method for the bottom-up synthesis of graphene nanoribbons longer than 200 nm.[14] However, this method might need to be adapted to the nature of the heteroatom or to its corresponding heterocycle. On one hand, Draper *et al.*[4] and Yamaguchi *et al.*[7] could use the cyclodehydrogenation for the preparation of their N- and B-containing PAHs. On the other hand, Müllen *et al.* and Nuckolls *et al.* used an alternative photocyclization method to access their S-containing PAHs.[15,16] In line, we recently developed a synthetic way toward P-containing PAHs based on this photochemical method.[17] This allowed us to use the reactivity of the P-atom to tune the optical properties as well as the supramolecular organization including the successful fabrication of a white light-emitting device (WOLED).[18] In the present article, we detail the different synthetic strategies allowing the preparation of these new P-containing PAHs. In particular, we detail how the classical synthetic methods have to be modified to the specificity of P-derivatives. The effect of the insertion of the P-atom at the edge was investigated by experimental (spectro-electrochemistry) and theoretical studies (aromaticity). The stable reduced species of the P-containing PAHs were studied in detail both experimentally and theoretically.

Results and discussions

As mentioned, the synthesis of PAHs usually proceeds with the cyclodehydrogenation of flexible polyaromatic synthons.[12] This synthetic approach was investigated with the star-shaped phosphole derivatives **2** (Scheme 1). This "graphenization" process generally involves excess of oxidants that are not compatible with the presence of a nucleophilic σ^3,λ^3-P center. Therefore, the usual Scholl conditions ($FeCl_3$, $MeNO_2$) were applied to the per-phenyl oxophosphole **2**, where the P-center is protected in its oxidized form, which was obtained via the Fagan-Nugent route from alkyne **1** followed by an oxidation in the presence of sodium periodate (Scheme 1). This Scholl reaction process led to over-oxidized compound **3** in which the phosphole ring is profoundly altered (Scheme 1). Note that the fate of the reaction is

similar using DDQ as oxidant.[19] The structure of derivative **3** was clearly established by multinuclear NMR spectroscopy, 2D experiments and high-resolution mass spectrometry (HRMS) and its NMR data fits with those reported for a similar P-ring.[20] The rather harsh reaction conditions (oxidant and acidic media) which are compatible with other heterocycles such as pyridines, cannot be used with the slightly antiaromatic[21] and consequently destabilized oxophosphole ring. The photocyclization method, which is a milder alternative and has already been used with phospholes (Scheme 1),[22] was thus investigated. After photocyclization of **2** during 4 days using the Katz-modified method,[23] a complicated reaction mixture was obtained from which only phosphole **4** (Scheme 1) could be isolated following column chromatography. Although the yield is low (5%), the synthesis of **4** is the first example of C-C bond formation between two phenyl substituents grafted on a phosphole ring.



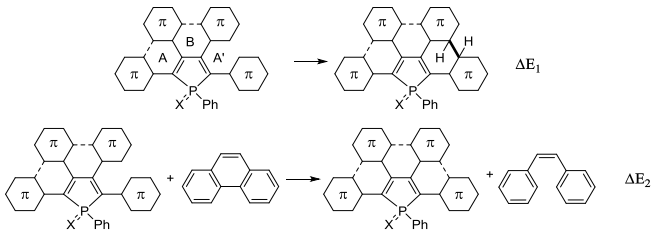
Scheme 1. Cyclization methods applied to the precursor **2** and **6**.

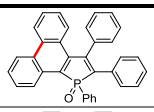
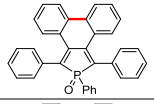
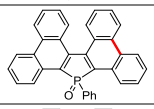
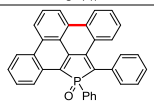
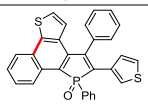
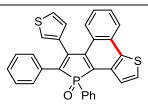
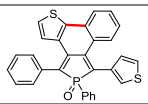
This result was encouraging and in order to favor the cyclization process, the photocyclization was conducted with phosphole **6** bearing consecutive phenyl- and thienyl-substituents (Scheme 1). This substitution pattern was obtained using the unsymmetrical alkyne **5** as starting material for the Fagan-Nugent synthesis (Scheme 2). Note that this reaction results in a statistic mixture of the three possible position isomers of **6**. The desired star-shaped derivative **6** was isolated in 20% yield following column chromatography. Remarkably, the photochemical method gave rise to derivative **7** resulting from the formation of two intramolecular C-C bonds in 52% isolated yield (Scheme 2). Having compound **7**, the last step towards the targeted PAH would be the formation of a C-C bond between the thienyl and phenyl rings at the 3,4-position of the P-heterole. This synthetic step could neither be achieved by chemical (Scholl reaction), nor by photochemical (Hg-lamp, I_2) methods. These unsuccessful approaches show that although the intramolecular C-C bond can be formed

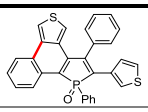
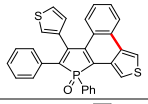
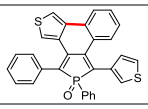
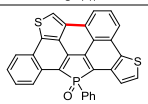
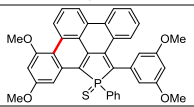
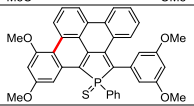
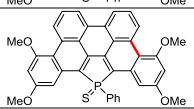
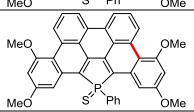
using the photochemical approach, the star-shaped phosphole **2** and **6** are not suitable starting materials for the preparation of P-containing PAHs. The low yields, as well as the difficulty of purification led us to modify our strategy.

To further investigate the reasons of the differences observed during the cyclization reactions, DFT calculations on **2H**, **4H**, **6H**, **7H**, **9a^{O,S}**, **10a^{O,S}** (Table 1 and Scheme 2) and their intermediates were used to get information on the energetics of the consecutive ring closure reaction steps.[24]

Table 1: B3LYP/6-31+G* reaction energies in kcal/mol. **6H$^{\alpha}$** and **6H$^{\beta}$** symbols refer to the ring closure of **6H** at the α or β position of the thienyl ring, respectively. The hexagon with the π symbol inside represents 6π-electron systems either in six or in five membered (thienyl) rings.



	FNR[b]		ΔE_1[c]	ΔE_2
2H[a]	A=A'		+38.3/+38.9	+4.4
	B		nmf[d]	+15.5
4H	A'		+40.5/+43.8	+7.5
	B		nmf	+9.2
6H$^{\alpha}$	A		+17.3/+17.3	-3.2
	A'		+20.0/+20.6	+1.0
	B		+50.0/nmf	+11.6

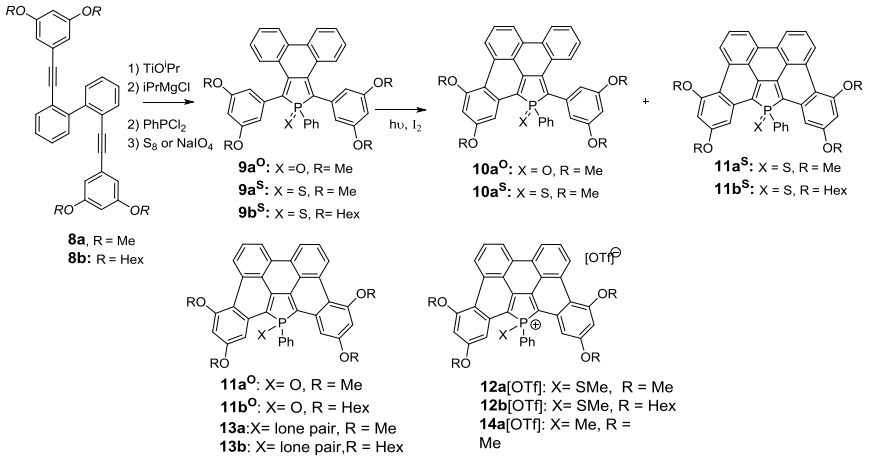
	FNR[b]		ΔE_1[c]	ΔE_2
6H$^{\beta}$	A		+51.9/+52.4	+3.4
	A'		+55.8/+57.0	+8.4
	B		nmf/nmf	+13.4
7H	B		nmf/nmf	+9.2
9a^{O}	A=A'		+26.1/+26.7	+0.5
9a^{S}	A=A'		+27.1/+27.5	+0.8
10a^{O}	A'		+30.7/+31.9	+3.9
10a^{S}	A'		+31.5/+31.9	+4.3

[a]XH refers to compound X with R = H. [b]FNR: Formation of the new ring at the A, B or A' position. [c] The second values correspond to the second trans isomer [d]nmf: no minima found

The ring closure reactions consist of two consecutive steps. In the first reaction (reaction energy ΔE_1 – Table 1) the new C-C bond is formed (with the hydrogens in trans position). The second reaction is a dehydrogenation process. Since the second step is facilitated by the presence of further reactants (hν, I_2), the absolute reaction energies are of little importance, therefore to investigate the overall process, the energetics are studied throughout using an isodesmic reaction, with reference to the ring-closure reaction of (Z)-stilbene forming a phenantrene (reaction energy ΔE_2 – Table 1). In general, the ring closure reaction energies (ΔE_1) are highly endothermic (apparently the energy of the photon is needed to complete this energetically unfavourable reaction step). Clearly, the closure of the B ring is thermodynamically less favourable than the closure of the A ring for all the investigated systems according to both the ΔE_1 and the ΔE_2 values. A likely reason of this is the larger steric congestion at these positions in the starting material. In accordance with the decreased stabilization upon ring closure between the aromatics at the 3- and 4-positions of the phosphole ring only one hydrogenated intermediate could be optimized for the closure of the B ring (Table 1). The comparison of the ring closure energetics between the thienyl substituted system **6H** (compound **6** with R = H) with the all phenyl substituted **2H** reveals the preferred formation of the new ring at the α-position of the thienyl ring, especially when the thienyl ring is at the β-position of the phosphole ring (closure of the A ring in **6H**). The closure of the B ring is endothermic in case of **6H** as well. It is noteworthy that once the B ring is closed the closure of the A and A' rings remains slightly exothermic in case of oxo- and thioxophospholes, with no significant difference between the different derivatives. (entries **9a^{O}-9a^{S}** and **10a^{O}-10a^{S}** in Table 1, Scheme 3).

Having all these information, it became evident that the precursor for the desired PAH formation should already possess a C-C link between the phenyl substituents at the 3,4-positions of the P-heterole (the B ring is already closed). Indeed, the suitable precursor **9** (Scheme 2) contains this key structural unit, furthermore O-alkyl substituents on the meta position of phenyl rings facilitate the formation of the C-C bond at the right position.[25] Following the synthetic strategy developed by Matano *et al.*,[26] dialkynes **8** (Scheme 2) were reacted in the Sato-Urabe conditions followed by oxidation with $NaIO_4$ or S_8 affording (thio)oxophospholes **9**. On this family of phospholes, the Sato-Urabe method allowed us to achieve better yield than our previously reported Fagan-Nugent synthesis. These air stable compounds display ^{31}P NMR chemical shift in the usual range for (thio)oxophospholes and all

their multinuclear NMR spectroscopic and mass spectrometry data confirmed the proposed structures.



Scheme 2. Synthetic access to P-containing polyaromatics **11** (up) and examples of their derivatives **12-14** (down)**.**

Since the over-oxidized compound **3** (Scheme 1) cannot be formed due to the specific design of the phospholes **9**, the chemical reactivity of these phospholes was tested in the Scholl conditions (with $FeCl_3$ or $MoCl_5$ in CH_2Cl_2). In all cases, the asymmetric phospholes **10** (Scheme 2) were rapidly formed but the fully cyclized product was never observed and degradation of the intermediate occurred within a few hours. We thus turned to the photocyclization method. The photocyclization of the oxophosphole **9a^O** gave rise to one major compound **10a^O** (^{31}P NMR, +39.6 ppm) resulting from the formation of one intramolecular C-C bond. This derivative was isolated in low yield (10%) (Scheme 2). Neither the increase of the reaction time nor the use of acid scavenger such as propylene oxide (PPO) allowed obtaining the desired **11a^O**. As oxophospholes are quite sensitive to acid (HI is produced during the photocyclization reaction), we envisaged that the reaction might be more efficient with **9a^S**, with a less polar P=S bond as protecting group. Indeed, the photocyclization produced two main compounds having ^{31}P NMR signals in the expected range. Both compounds were separated by chromatography on silica gel and identified as **11a^S** (^{31}P NMR, +46.0 ppm; yield: 20%) and **10a^S** (^{31}P NMR, +51.6 ppm yield: 50%) (Scheme 2). With this strategy, two P-containing PAHs **11a-b^S** were synthesized, fully characterized and isolated as air stable derivatives. This reactivity study shows how the design of the precursor is a key parameter toward the preparation of P-containing PAHs. In particular, steric factor clearly appears as very influent parameter. However, electronic

parameters and chemical stability are also important as evidenced by the synthesis of **3** and the difference of reactivity between **9a^{O}** and **9a^{S}**.

Our reported strategy of P-functionalization was also efficient on the soluble P-containing PAHs bearing long aliphatic chains **11b**.[18] Starting from the PS protected σ^4,λ^5-P-derivative **11b^{S}**, its σ^3,λ^3-P-analogue **13b** and its oxidized analog **11b^{O}** could be prepared; as well as the phospholium **12b**[OTf]. It is important to note that these derivatives cannot be obtained directly through the photocyclization method from the corresponding derivative of **9**. As suggested by the different chemical shifts observed in the ^{31}P NMR (see SI), the electronic deficiency of σ^4,λ^5- and σ^4,λ^4-phosphole derivatives can be modulated by the nature of the substituents introduced on the P-atom.

The optical properties of the dibenzophosphapentaphenes **11**-**14** were first investigated by means of UV-Vis absorption and fluorescence measurements in dichloromethane (Table S1 of the Supporting Information).[17] As previously observed, the modulation of the electronic density on the P-atom allows the tuning of the absorption in the visible range, as evidenced in Fig. 1 left with **11a^{S}** and **14a**[OTf]. Furthermore **11a^{S}** and **14a**[OTf], which present a reversible first reduction process (Table S1 of the Supporting Information), were studied by spectro-electrochemistry. Their UV/Vis/NIR absorption properties upon oxidation/reduction were investigated in an optically transparent thin-layer electrochemical cell (OTTLE). The one electron reduction of **11a^{S}** and **14a**[OTf] led to a decrease in the intensities of their 514 and 554 nm bands, respectively and a new vibrationally structured absorption band appeared in the visible and near-infra-red regions (Fig. 1 right) at lower energies. The regeneration of the starting material by reversing the potential (Fig. S1-2 of the Supporting Information) shows the reversibility of this reduction process. The absorption spectrum upon oxidation for **11a^{S}** was also recorded (Fig. S4 of the Supporting Information). In this case, the structured band at 514 nm of **11a^{S}** is converted to a large and unstructured band centered at 585 nm. The oxidized species were found unstable at ambient temperatures as witnessed by the absorption spectrum failing to return to that of the parent species on re-reduction of the solution and as expected from the CV measurements (Table S1 of the Supporting Information).

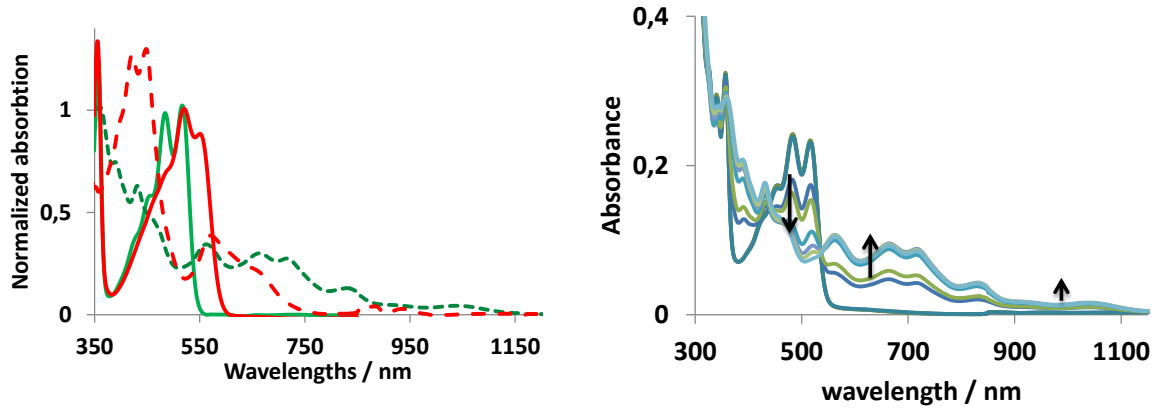


Fig. 1. Absorption spectra of phospholes **11a**^{S} (green) and **14a**[OTf] (red) and their respective first isolated reduction states (dashed) (left). UV-Vis absorption changes of **11a**^{S} upon reduction (right) (measured in 0.2 M NBu_4PF_6 dichloromethane solution, c = 10^{-4} M).

Calculation of the one electron oxidized and reduced structures of **11a**^{S} and **14a**[OTf] show that the cation formation from **11a**^{S} and from **14a**[OTf] are energetically demanding, while the corresponding anions exhibit positive electron affinity, in accordance with the observed stability of the reduced form.

To deepen our understanding of the effect of chemical modifications performed on the P-atom on the physical properties, **11a**^{S,O}, **12a**$^{+}$, **12a**[OTf], **13a**, **14a**$^{+}$ and **14a**[OTf] were investigated computationally. Representation of HOMO-LUMO orbitals are presented in SI (Fig. S7 of the Supporting Information), showing the delocalization about the entire π-system, including the phosphole ring. To investigate the aromaticity NICS,[27,28,29] Bird unified aromaticity index[30] and BDSHRT[31] values were calculated for all the rings in **11a**^{O}, **11a**^{S}, **12a**$^{+}$, **13a** and **14a**$^{+}$ and are compiled in Tables S3-5 of the SI. Among these aromaticity measures the NICS(1) values, which describe antiaromaticity as well, are shown schematically in Fig. 2 (NICS(0) – as expected - displays similar trend). The local aromaticity values in the five membered rings are in good accordance with the relative aromaticities of the P-substituted parent phospholes, the cationic systems exhibiting the largest antiaromaticity.[21,32] The same aromaticity trend is supported by the experimental ^{13}C NMR shifts of the carbon at the α position of the phosphole ring (see Table S6 of the Supporting Information). It is noteworthy that as we have noted before on the dibenzo[fg,ij]pentaphene model system,[33] the variation of the aromaticity in the five membered ring affects considerably the aromaticity in the endocyclic six – membered ring. In accordance, in case of **11a**^{O}, **11a**^{S}, **12a**$^{+}$, and **14a**$^{+}$ positive (antiaromatic) NICS values were obtained even in the

embedded six-membered ring. Thus, the modifications at the P do not only act locally, but have an impact on the entire π-system as well.

It should be noted that the increase in the antiaromatic character in the five-membered ring is in good accordance with the decrease of the HOMO-LUMO gap, and the most antiaromatic compounds show the largest red-shift in absorption. The TD-DFT calculated vertical excitation energies are in good agreement with the absorption spectra for the neutral molecules, and also for the cationic systems if the counter anion (OTf^-) is explicitly considered (Table S8 of the Supporting Information). This behavior suggests that in solution the positive and negative ions form a tight ion pair. Using TD-DFT geometry optimization, we also calculated the vertical emission energies. While these show less satisfactory agreement with the experimental data than the calculated absorption band maxima, the tendencies in the Stokes shifts are clearly reproduced, the cationic systems exhibiting significantly larger red shifts than the neutral molecules. In the excited state, a significant equalization of the C-C bonds of the phosphole unit is always observed (Table S7 of the Supporting Information), in accordance with the variation of the bonding and antibonding characters of the HOMO and LUMO – see below. However, no clear trend of bond length alternation depending on P-environment could be made. PCM calculations were also carried out to estimate solvent effects, but no significant difference from the gas phase results was obtained (Comparison between the methods is summarized in Table S8 of the Supporting Information).

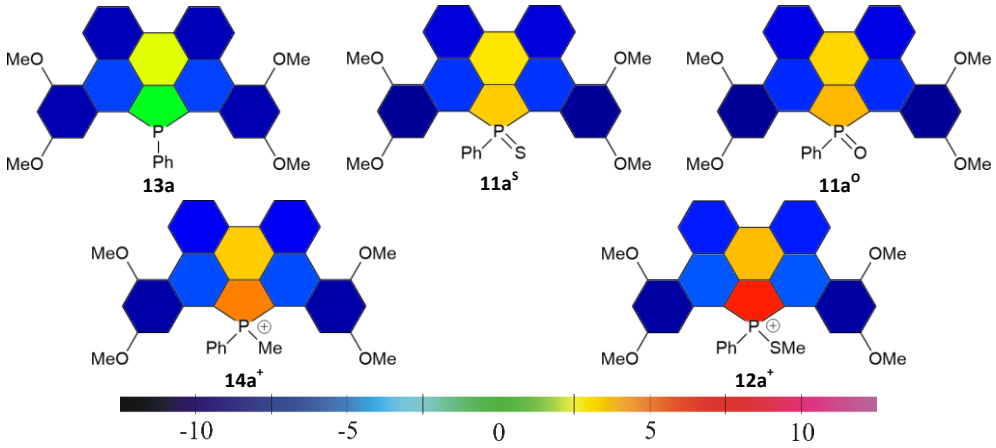


Fig. 2. Schematic representation of the NICS(1) results for **11a**^{S,O}, **12a**$^{+}$, **13a**, **14a**$^{+}$. The black circle represents antiaromatic and gray circle represents aromatic ring current, the size of the ring is proportional to the calculated shielding.

The ground-state electronic structure of the neutral, oxidized and reduced form of compounds **11a**^{S}, **14a**$^{+}$, **14a**[OTf] have also been investigated. The SOMO orbitals can be derived from the corresponding orbitals of the neutral species, in case of oxidation, the former HOMO and in case of reduction the former LUMO, respectively. (Fig. 3) The geometry of the radicals shows equalization of the C-C bonds of the phosphole unit, similarly to the effect of the HOMO-LUMO excitation, in good agreement with the shape of the SOMO orbitals, where in case of oxidation there is only one electron occupying the former HOMO, therefore the double-bonds weaken, and in case of reduction the former LUMO has an electron, which strengthens the C-C bond in the 3-4 position of the phosphole. The equalization is more pronounced in case of the reduced forms (**11a**^{S}•$^{-}$ and **14a**$^{•}$) (Table S9 of the Supporting Information). The TD-DFT calculations on the doublet state of the radicals correspond well with the red-shifted absorption spectra (Table S11 of the Supporting Information) and predict that the absorption bands correspond to $\pi-\pi*$ transitions. NICS(1) aromaticity studies carried out on the radicals (both oxidized and reduced species) show strengthening of the aromatic character both in the phosphole and in the endocyclic rings, in agreement with the bond length equalization. (Table S10 of the Supporting Information and Fig. 4)

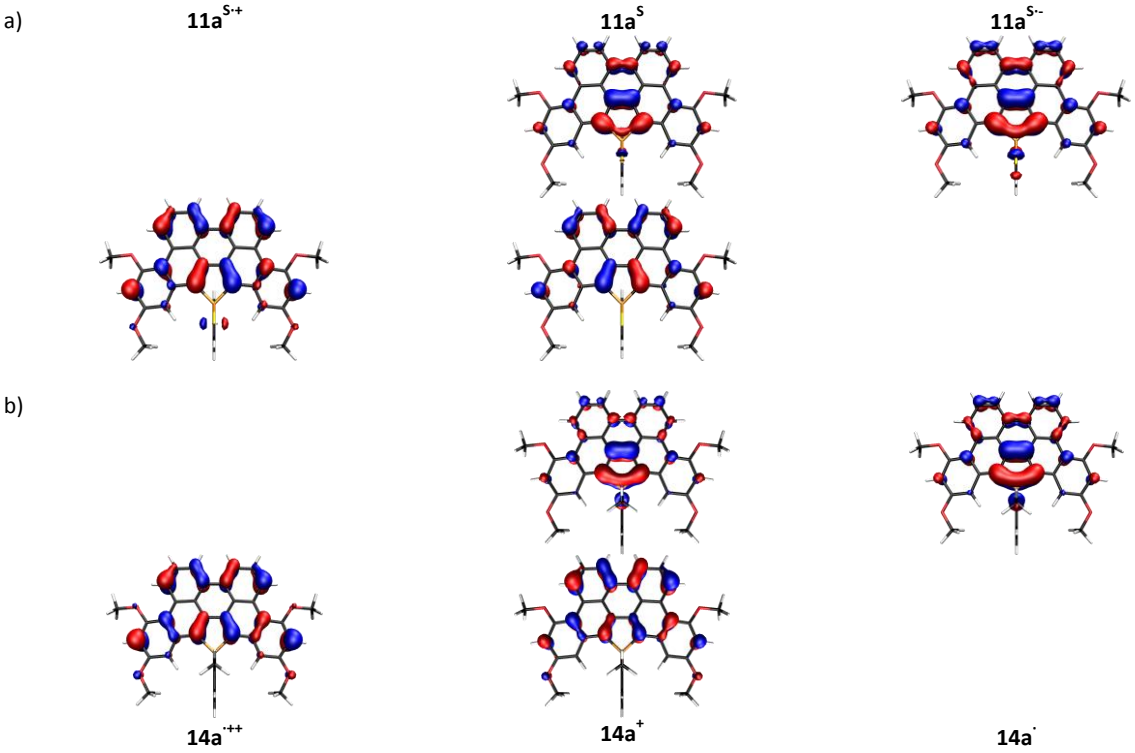


Fig. 3. Comparison of SOMO orbitals in oxidized (left) and reduced (right) species of **11a**^{S} (a) and **14a**$^{+}$ (b) and the FMOs of **11a**^{S} and **14a**$^{+}$ at the B3LYP/6-31+G* level

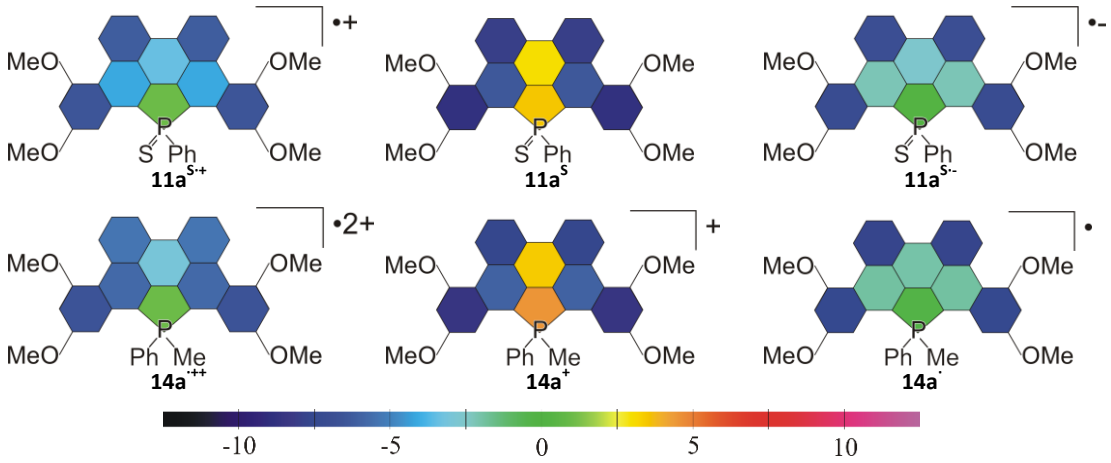


Fig. 4. Schematic representation of the NICS(1) results for oxidized (left) and reduced (right) species of **11a**^{S} (a) and **14a**$^{+}$ (b)

Conclusion

In conclusion, the synthetic strategy that allowed us to insert a reactive σ^3,λ^3-P atom into a 2D π-conjugated framework has been detailed with experimental and theoretical data. The P-modified PAHs **13a-b** possess the classical reactivity of phosphane compounds that allows to fine tune the electronic properties of these compounds as evidenced by UV-Vis absorption,

and theoretical calculations. Interestingly, theoretical calculations showed that the presence of the P-atom impacts the local aromaticity of several rings, in particular that of the endocyclic 6-membered ring. The reduced species of the PAHs were stable enough to be studied by spectro-electrochemistry and the results were rationalized by DFT calculations. Investigation of the coordination ability of this PAH based P-ligand is currently under investigation as well as their incorporation into opto-electronic devices.[34, 35]

Experimental Section

*General Procedures***.** All experiments were performed under an atmosphere of dry argon using standard Schlenk techniques. Commercially available reagents were used as received without further purification. Solvents were freshly purified using MBRAUN SPS-800 drying columns. Irradiation reactions were conducted using a Heraeus TQ 150 mercury vapor lamp. Separations were performed by gravity column chromatography on basic alumina (Aldrich, Type 5016A, 150 mesh, 58 Å) or silica gel (Merck Geduran 60, 0.063-0.200 mm). ^{1}H, ^{13}C, and ^{31}P NMR spectra were recorded on a Bruker AM300, AM400, AM500. ^{1}H and ^{13}C NMR chemical shifts were reported in parts per million (ppm) relative to Me_4Si as external standard. Assignment of proton and carbon atoms is based on COSY, HMBC, HMQC and DEPT-135 experiments. High-resolution mass spectra were obtained on a Varian MAT 311 or ZabSpec TOF Micromass instrument at CRMPO, University of Rennes 1. Elemental analyses were performed by the CRMPO, University of Rennes 1. Compounds **1**, **5**, **8a-b**, **9a-b**^{S,O,} **11a**^{S}**,O**, **11b**^{S}, **12-14a**, were synthesized according to published procedure.[17,18, 36, 37]. UV/vis/NIR spectroelectrochemistry (SEC) experiments were performed in freshly distilled dichloroethane (0.2 M Bu_4NPF_6), under argon, with optically transparent thin-layer electrosynthetic (OTTLE) cell, path length 1mm, using a Varian CARY 5000 spectrometer and an EG&G PAR Model 362 potentiostat. Pt mesh was used as the working electrode, Pt wire as the counter electrode, and Ag wire as a pseudoreference electrode. The electrodes were arranged in the cell such that the Pt mesh was in the optical path of the quartz cell.

Compound **2**. 1,2-Bis(4-butylphenyl)ethyne **1** (300 mg, 1.03 mmol) and $ZrCp_2Cl_2$ (151.2 mg, 0.52 mmol) were dissolved in dry THF (15 mL), then a solution of n-BuLi (2.5M, 0.44 mL, 1.09 mmol) is added dropwise at -78°C. After stirring overnight at room temperature (RT), the solution is cooled at 0°C and CuCl (102 mg, 1.03 mmol) was then added. The solution is stirred for 1 h. Then, $PhPCl_2$ (0.1 mL, 0.7 mmol) is added to solution and stirred for 1 h at

0°C. The solution is warmed to RT and stirred for an additional 24 h. The solution is filtered on basic alumina and the solvent were evaporated. The σ^3,λ^3-phosphole (^{31}P NMR (160 MHz, CDCl3): δ = +16.1 ppm) is then oxidized with excess $NaIO_4$ in a biphasic solution CH_2Cl_2/H_2O for 30 mn. The organic layer is dried on $MgSO_4$, then evaporated and the crude mixture is purified by chromatography on silica gel using n-heptane : diethyl ether (1:1, v/v) as eluent to afford **2** as a yellow solid (286 mg, 78%). ^{1}H NMR (400 MHz, $CDCl_3$) : δ 0.84-0.92 (m, 12H, CH_3) ; 1.21-1.31 (m, 8H, CH_2CH_3) ; 1.44-1.56 (m, 8H, $CH_2C_2H_5$) ; 2.49 (m, 8H, $CH_2C_3H_7$); 6.83 (d, 4H, ^3J(H,H) = 8.3 Hz, H_{phenyl}); 6.87 (d, 4H, ^3J(H,H) = 8.3 Hz, H_{phenyl}); 6.93 (d, 4H, ^3J(H,H) = 8.3 Hz, H_{phenyl}) 7.08 (d, 4H, ^3J(H,H) = 8.3 Hz, H_{phenyl}) ; 7.41-7.47 (m, 3H, H_{meta} and H_{para}) ; 7.95 (ddd, 2H, ^4J(H,H) = 2 Hz, ^3J(H,H) = 8 Hz, J(P,H) = 14 Hz, H_{ortho}). ^{13}C NMR ($CDCl_3$, 75.5 MHz) : δ 13.9 (s, CH_3) ; 14.0 (s, CH_3) ; 22.0 (s, CH_2CH_3) ; 22.4 (s, CH_2CH_3) ; 33.1 (s, $CH_2CH_2CH_3$) ; 33.3 (s, $CH_2CH_2CH_3$) ; 35.3 (s, $C_3H_7CH_2$-Ph) ; 35.4 (s, $C_3H_7CH_2$-Ph) ; 128.1 (s, CH_{phenyl}) ; 128.2 (s, CH_{phenyl}) ; 128.9 (d, J(P,C) = 12 Hz, CH_{meta}) ; 129.1 (d, J (P,C) = 6 Hz, CH_{phenyl}) ; 129.4 (s, CH_{phenyl}) ; 130.0 (d, J (P,C) = 12 Hz, C_{phenyl}) ; 130.3 (d, J (P,C) = 93 Hz, C_{ipso}) ; 130.7 (d, J (P,C) = 10.6 Hz, C_{ortho}) ; 131.7 (d, J (P,C) = 3 Hz, CH_{para}) ; 133.7 (d, J (P,C) = 92.9 Hz, Cα) ; 132.8 (d, J (P,C) = 17 Hz, C_{phenyl}) ; 142.4 (s, C_{phenyl}-C_4H_9); 150.0 (d, J (P,C) = 27 Hz, $C_β$). ^{31}P NMR ($CDCl_3$, 121.5 MHz) : δ +44.4. Anal calcd for $C_{50}H_{57}OP$: C 85.19, H 8.15 ; Found : C 85.12, H 8.12. HR-MS (EI, CH_2Cl_2/MeOH, 9/1, m/z): [M]+ calcd for $C_{50}H_{57}OP$: 705.4225; found: 705.4227.

Compound **3**. Compound **2** (130 mg, 0.18 mmol, 0.01 mol/L) in dry CH_2Cl_2 (43 mL) and a solution of iron chloride (III) (598 mg, 7.69 mmol) in nitromethane (8 mL) are sparged with argon. The ferric solution is added dropwise to the phosphole solution. The black reaction mixture is stirred for 18 days with successive additions of iron and CH_2Cl_2. The organic phase is washed with water (20x50 mL) to extract the iron excess, then dried over $MgSO_4$ and the solvents are removed. The product is purified on silica gel chromatography (n-heptane/ethyl ether, v/v 99/1→ 95/5) to afford **3** as a yellow solid (27 mg, 20%). 1H NMR (400 MHz, CD_2Cl_2) : δ 0.89-0.99 (m, 12H, CH_3) ; 1.21-1.43 (m, 8H, CH_2CH_3) ; 1.44-1.50 (m, 2H, $CH_2C_2H_5$) ; 1.53-1.58 (m, 2H, $CH_2C_2H_5$); 1.60-1.69 (m, 4H, $CH_2C_2H_5$) ; 2.47 (t, 2H, ^3J(H,H) = 8 Hz, $CH_2C_3H_7$) ; 2.58 (t, 2H, ^3J(H,H) = 8 Hz, $CH_2C_3H_7$) ; 2.64 (t, 2H, ^3J(H,H) = 8 Hz, $CH_2C_3H_7$) ; 2.68 (t, 2H, ^3J(H,H) = 8 Hz, $CH_2C_3H_7$) ; 6.87 (d, 2H, ^3J (H,H) =8 Hz, H_{phenyl}); 7.05 (d, 2H, ^3J(H,H) = 8 Hz, H_{phenyl}); 7.09 (d, 2H, ^3J(H,H) = 8 Hz, H_{phenyl}); 7.16 (d, 2H, ^3J (H,H) =8 Hz, H_{phenyl}); 7.21 (d, 2H, ^3J (H,H) = 8 Hz, H_{phenyl}); 7.24 (d, 2H, ^3J (H,H) = 8 Hz, H_{phenyl}); 7.29 (d, 2H, ^3J (H,H) = 8 Hz, H_{phenyl}); 7.25-7.27 (m, 2H, H_{meta}) ; 7.36-7.40 (m, 1H,

H_{para}); 7.45 (ddd, 2H, ^{4}J (H,H) = 2 Hz, ^{3}J (H,H) = 8 Hz, J (P,H) = 14 Hz, H_{ortho}); 7.65 (d, 2H, ^{3}J (H,H) =8 Hz, H_{phenyl}). ^{13}C NMR (125 MHz, CD_2Cl_2) : δ 13.6 (s, CH_3); 13.7 (s, CH_3); 13.8 (s, CH_3); 13.9 (s, CH_3) ; 21.9 (s, CH_2CH_3); 22.3 (s, CH_2CH_3); 22.4 (s, CH_2CH_3); 22.7 (s, CH_2CH_3) ; 33.2 (CH_2-C_2H_5) ; 33.4 (large s, CH_2-C_2H_5, CH_2-C_2H_5); 34.9 (s, CH_2-C_3H_7); 35.1 (s, CH_2-C_3H_7); 35.4 (s, CH_2-C_3H_7); 35.5 (CH_2-C_3H_7); 64.2 (d, J(P,C) = 69 Hz, Cα) ; 128.0 (s, CH_{phenyl}) ; 128.2 (d, J (P,C) = 11.3 Hz, CH_{meta}) ; 128.5 (s, CH_{phenyl}) ; 128.7 (d, J(P,C) = 29 Hz, CH_{phenyl}) ; 128.9 (d, J (P,C) =20 Hz, C_{phenyl}) ; 129.0 (s, C_{phenyl}) ; 129.3 (d, J (P,C) =5 Hz, CHphenyl) ; 129.7 (large s, 2 CHphenyl) ; 130.0 (d, J (P,C) = 5 Hz, CH_{phenyl}) ; 130.4 (d, J(P,C) = 5 Hz, CH_{phenyl}) ; 130.7 (d, J(P,C) =106 Hz, C_{ipso}) ; 131.6 (d, J(P,C) = 9 Hz, C_{Hortho}) ; 131.7 (d, J(P,C) = 2 Hz, CH_{para}) ; 133.7 (s, C_{phenyl}) ; 135.7 (d, J (P,C) = 2 Hz, C_{phenyl}) ; 141.5 (d, J (P,C) = 2 Hz, C_{phenyl}) ; 142.3 (s, C_{phenyl}) ; 144.6 (s, C_{phenyl}); 145.8 (s, C_{phenyl}) ; 150.6 (d, J (P,C) =23 Hz, Cβ) ; 150.8 (d, J (P,C) = 59 Hz, Cα) ; 195.1 (d, J (P,C) = 25 Hz, Cβ) ; ^{31}P NMR (121.5 MHz, CD_2Cl_2): δ +41.9 ; HR MS (ESI, CH_2Cl_2/MeOH, 9/1, m/z): $[M+Na]^+$ calcd for $C_{50}H_{57}O_2PNa$: 743.39884, Found: 743.3988.

Compound **4**. Compound **2** (90 mg, 0.128 mmol) was dissolved in toluene (200 mL) with a catalytic amount of I_2 (20 mg). The solution is irradiated for 68 h UV light using a Heraeus TQ 150 mercury vapor lamp. All volatile materials were removed under vacuum and the product is purified on silica gel chromatography (dichloromethane) to afford 4 as a yellow solid (5%). 1H NMR (400 MHz, CD_2Cl_2) : δ 0.92 (t, 3H, ^{3}J(H,H) = 8 Hz, CH_3) , 0.99 (t, 3H, ^{3}J(H,H) = 8 Hz, CH_3) ; 1.00 (t, 3H, ^{3}J(H,H) = 8 Hz, CH_3) ; 1.03 (t, 3H, ^{3}J (H,H) = 8 Hz, CH_3) ; 1.45 (m, 8H, CH_2CH_3) ; 1.73 (m, 8H, $CH_2C_2H_5$) ; 2.51 (t, 2H, ^{3}J(H,H) = 8.0 Hz, $CH_2C_3H_7$) ; 2.78 (t, 2H, ^{3}J(H,H) = 8 Hz, $CH_2C_3H_7$) ; 2.86 (t, 2H, ^{3}J(H,H) = 8.0 Hz, $CH_2C_3H_7$) ; 2.89 (t, 2H, ^{3}J(H,H) = 8 Hz, $CH_2C_3H_7$) ; 6.95 (d, 2H, ^{3}J(H,H) = 8 Hz, CH_{phenyl}); 7.06 (d, 2H, 3J(H,H) = 8 Hz, CH_{phenyl}); 7.11 (dd, ^{1}H, ^{3}J(H,H) = 8.7 Hz, J(P,H) = 1.7 Hz, CH_{phenyl}) ; 7.33 (m, 4H, CH_{phenyl}); 7.36 (d, 1H, 3J(H,H) = 8.7 Hz, CH_{phenyl}); 7.40-7.47 (m, 3H, H_{meta}) ; 7.49-7.52 (m, 1H, H_{para}); 7.90 (ddd, 2H, ^{4}J(H,H) = 2 Hz, ^{3}J(H,H) = 8 Hz, J(P,H) = 14 Hz, H_{ortho}); 8.15 (d, 1H, ^{3}J(H,H) = 8.3 Hz, CH_{phenyl}) ; 8.52 (s, 1H, CH_{phenyl}) ; 8.58 (d, 1H, ^{4}J(H,H) = 1.5 Hz, CH_{phenyl}).^{31}P NMR (121.5 MHz, CD_2Cl_2) : δ +41.9 (s); HR-MS (ESI, CH_2Cl_2/MeOH, 9/1, m/z): [M+Na]+ calcd for $C_{50}H_{55}OPNa$: 725.3888; found: 725.3879.

Compound **6**. Derivative **5** (0.170 g, 0.7 mmol, 1 eq.) and Cp_2ZrCl_2 (103 mg, 1 eq.) were dissolved in THF (30 mL), and then n-BuLi (2.5 M, 0.29 mL, 2.1 eq.) was added dropwise at -78°C. The solution was warmed at RT and stirred 24 h. At 0°C, CuCl (73 mg, 2.1 eq.) was

added and the solution was stirred for 1h at this temperature, then $PhPBr_2$ (0.06 mL, 1.2 eq.) was added. The solution was warmed at RT and stirred for 24 h. The solution was filtered on basic alumina and the solvent were evaporated. The orange precipitate of σ^3,λ^3-phosphole was dissolved in dichloromethane (30 mL), an excess of $NaIO_4$ and 0.1 mL of water were added and the solution was stirred for 3 h. The solution was washed with water, dried on MgSO4 the solvent was evaporated. The crude precipitate was purified by chromatography on silica gel using dichloromethane as eluent to afford 6 as an orange solid (30 mg, 20 %).1H NMR (400 MHz, CD_2Cl_2,) : 0.67 (t, 3H, ^3J (H,H) = 8 Hz, CH_3) ; 0.94 (t, 3H, ^3J (H,H) = 8 Hz, CH_3); 1,30-1.40 (m, 4H, C_2H_4-CH_2- CH_3) ; 1.45-1.55 (m, 2H, CH_2-CH_2-C_2H_5) ; 1.55-1.70 (m, 2H, CH_2-CH_2-C_2H_5) ; 2.54 (t, 2H, ^3J (H,H) = 8 Hz, CH_2-C_3H_7) ; 2.68 (t, 2H, ^3J (H,H) = 8 Hz, CH_2-C_3H_7) ; 6.65 (ddd, ^{1}H, J (H,H) = 5 Hz, J (H,H) = 1 Hz, J (P,H) = 1 Hz, $H_{thienyl}$); 6.67 (dd, 1H, ^3J (H,H) = 6 Hz, 4J (H,H) = 2 Hz, $H_{thienyl}$); 6.83 (ddd, 1H, J (H,H) = 3 Hz, J (H,H) = 1 Hz, J (P,H) = 1 Hz, $H_{thienyl}$); 7.00 (d, 2H, ^{3}J (H,H) = 8 Hz, H_{phenyl}); 7.05 (d, 2H, ^{3}J (H,H) = 8 Hz, H_{phenyl}); 7.05-7.10 (m, 1H, $H_{thienyl}$); 7.13-7.16 (m, 3H, $H_{thienyl}$ and H_{phenyl}); 7.19 (d, 2H, ^3J (H,H) = 8 Hz, H_{phenyl}); 7.27 (m, 1H, $H_{thienyl}$); 7.45-7.55 (m, 3H, H_{para} and H_{meta}); 7.93 (ddd, 2H, ^4J (H,H) = 2 Hz, ^{3}J (H,H) = 8 Hz, J(P,H) = 14 Hz, H_{ortho}). ^{13}C NMR (125 MHz, CD_2Cl_2) : 13.6 (s, CH_3) ; 13.7 (s, CH_3) ; 22.2 (s, CH_2- CH_3); 22.4 (s, CH_2-CH_3); 33.3 (s, CH_2-C_2H_5) ; 33.4 (s, CH_2-C_2H_5); 35.3 (s, CH_2-C_3H_7) ; 35.4 (s, CH_2-C_3H_7); 124.9 (s, $CH_{thienyl}$); 125.0 (s, $CH_{thienyl}$); 125.5 (d, J(P,C) = 6 Hz, $CH_{thienyl}$); 125.9 (s, $CH_{thienyl}$); 127.1 (d, J(P,C) = 7 Hz, $CH_{thienyl}$); 128.1 (d, J(P,C) = 70 Hz, C_{ipso}); 128.3 (s, CH_{phenyl}); 128.6 (s, CH_{phenyl}); 128.7 (s, CH_{phenyl}); 128.9 (s, $CH_{thienyl}$); 129.0 (s, CH_{phenyl}) ; 129.1 (d, J(P,C) = 10 Hz, CH_{meta}); 129.4 (d, J(P,C) = 70 Hz, Cα); 130.1 (d, J(P,C) = 10 Hz, C_{phenyl}); 130.6 (d, J(P,C) = 10 Hz, CH_{ortho}); 132.0 (d, J(P,C) = 3 Hz, CH_{para}); 132.5 (d, J(P,C) = 91 Hz, Cα); 133.1 (s, C_{phenyl}); 133.32 (d, J(P,C) = 7 Hz, $C_{thienyl}$); 135.2 (d, J(P,C) = 15 Hz, $C_{thienyl}$); 143.1 (s, C_{phenyl}); 143.4 (s, C_{phenyl}),145.2 (d, J(P,C) = 30 Hz, Cβ); 148.4. (d, J(P,C) = 25 Hz, Cβ). 31P NMR (121.5 MHz, CD_2Cl_2,): +43.3. HR-MS (ESI, CH_2Cl_2/MeOH, 9/1, m/z): [M]+ Calcd for $C_{38}H_{37}OPS_2$: 604.2023 ; found : 604.2029.

Compound **7**. Derivative **6** (40 mg, 0.06 mmol) was dissolved in toluene (300 mL) with a catalytic amount of I_2 (5 mg). The solution is irradiated for 24 h with UV light using a Heraeus TQ 150 mercury vapor lamp. All volatile materials were removed under vacuum and the product is purified on silica gel chromatography (heptane then a gradient of diethyl ether) to afford **7** as a yellow solid (19 mg, 52%). ^{1}H NMR (400 MHz, CD_2Cl_2,) : 0.95 (t, 3H, ^3J (H,H) = 8 Hz, CH_3) ; 1.05 (t, 3H, ^3J (H,H) = 8 Hz, CH_3) ; 1,40-1.50 (m, 4H, CH_2-CH_3) ; 1.76

(m, 2H, CH_2-C_2H_5) ; 1.85 (m, 2H, CH_2-C_2H_5) ; 2.88 (t, 2H, ^3J (H,H) = 8 Hz, CH_2-C_3H_7) ; 2.96 (t, 2H, ^3J (H,H) = 8 Hz, CH_2-C_3H_7) ; 7.35 (m, 2H, H_{meta}) ; 7.45 (d, 1H, ^3J (H,H) = 8 Hz, H_{phenyl}); 7.48 (m, 1H, H_{para}) ; 7.56 (dd, 1H, ^3J (H,H) = 8 Hz, ^4J (H,H) = 2 Hz, H_{phenyl}); 7.64 (d, 1H, ^{3}J (H,H) = 6 Hz, $H_{thienyl}$) ; 7.66 (d, 1H, ^3J (H,H) = 6 Hz, $H_{thienyl}$) ; 7.74 (d, 1H, ^3J (H,H) = 6 Hz, $H_{thienyl}$) ; 7.80 (ddd, 2H, ^{4}J (H,H) = 2 Hz, ^3J (H,H) = 8 Hz, J(P,H) = 14 Hz, H_{ortho}); 7.94 (d, 1H, ^3J (H,H) = 6 Hz, $H_{thienyl}$) ; 8.07 (s, 1H, H_{phenyl}); 8.10 (s, 1H, H_{phenyl}); 8.20 (d, 1H, ^3J(H,H) = 8 Hz, H_{phenyl}) ; 8.55 (d, 1H, ^3J(H,H) = 8 Hz, H_{phenyl}). ^{13}C NMR (125 MHz, CD_2Cl_2) : 13.7 (s, CH_3) ; 13.8 (s, CH_3) ; 22.4 (s, CH_2-CH_3); 22.5 (s, CH_2-CH_3) ; 33.4 (s, CH_2-C_2H_5) ; 33.5 (s, CH_2-C_2H_5) ; 35.8 (s, CH_2-C_3H_7) ; 35.9 (s, CH_2-C_3H_7); 122.8 (s, $CH_{thienyl}$); 122.9 (s, CH_{phenyl}); 123.4 (s, $C_{Hphenyl}$); 124.1 (d, J(P,C) = 11 Hz, C_{phenyl}) ; 125.0 (s, $CH_{thienyl}$); 126.1 (d, J(P,C) = 5 Hz ; CH_{phenyl}) ; 126.7 (s, CH_{phenyl}) ; 127.3 (s, $CH_{thienyl}$); 127.8 (s, $CH_{thienyl}$) ; 127.9 (d, J(P,C) = 104 Hz, Cα) ; 128.5 (s, CH_{phenyl}); 128.9 (d, J(P,C) = 12 Hz, CH_{meta}) ; 129.1 (s, CH_{phenyl}) ; 129.2 (d, J(P,C) = 104 Hz, Cα) ; 129.6 (s, C_{phenyl}); 130.9 (d, J(P,C) = 10 Hz, CH_{ortho}) ; 131.1 (d, J(P,C) = 100 Hz, C_{ipso}); 132.2 (d, J(P,C) = 4 Hz, CH_{para}) ; 132.7 (s, C_{phenyl}) ; 132.9 (d, J(P,C) = 12 Hz, $C_{thienyl}$); 135.0 (d, J(P,C) = 10 Hz, $C_{thienyl}$); 135.8 (s, $C_{thienyl}$); 138.9 (d, J(P,C) = 20 Hz, Cβ) ; 139.2 (d, J(P,C) = 10 Hz, C_{phenyl}) ; 139.9 (d, J(P,C) = 15 Hz, Cβ) ; 143.0 (s, C_{phenyl}) ; 144.1 (s, C_{phenyl}) ; 144.4 (s, $C_{thienyl}$). ^{31}P NMR (160 MHz, CD_2Cl_2): δ +34.6 (s). HR-MS (ESI, CH_2Cl_2/MeOH, 9/1, m/z): [M+Na]+ Calcd for $C_{38}H_{33}ONaPS_2$: 623.16082 ; found : 623.1603.

Compound **9a^S**. Compound **8a** (500 mg, 1.26 mmol, 1 eq.) and $Ti(OiPr)_4$ (393 mg, 1.1 eq.) were dissolved in Et_2O (30 mL), then ^{i}PrMgCl (1.5 M, 1.8 mL, 2.2 eq.) was added dropwise at -78°C. The solution was warmed at RT and stirred 1 h. To this solution was added $PhPCl_2$ (0.2 mL, 1.2 eq.) at -78°C. The solution was warmed at RT and stirred for 24 h. The solution was evaporated, dissolved in DCM then filtered on basic alumina and the solvent were evaporated. The orange precipitate was dissolved in dichloromethane (30 mL), an excess of S_8 and 0.1 mL of triethylamine were added and the solution was stirred for 3 h. The solution was filtered and the solvent was evaporated. The crude precipitate was purified by chromatography on silica gel using dichloromethane as eluent to afford 9aS as an orange solid (460 mg, 60 %). The NMR data fit with our previously reported method.[17]

Compound **12b**[OTf]. At -80°C, to a 20 mg solution of compound **11b^S** in 15 mL of dichloromethane are added 2.8 µL (1.1 eq) of methyl triflate. After stirring of the solution overnight at RT, compound **12b**[OTf] is obtained after evaporation of solvent and washing

with pentane in 80% yield as 19 mg of a dark-purple solid. ^{1}H NMR (300 MHz, $CDCl_3$): δ 0.93 (t, ^{3}J (H,H) = 6 Hz, 12H, CH_3); 1.20-1.50 (m, 16H, CH_2) 1.55-1.65 (m, 8H, CH_2); 1.75-1.85 (m, 4H, CH_2); 2.05-2.15 (m, 4H, CH_2); 2.33 (d, 3H, ^{3}J (P,H) = 16 Hz, $PSCH_3$); 3.79-4.32 (m, 8H, O CH_2); 6.75-6.85 (m, 4H, CH_{phenyl}); 7.67-7.92 (m, 5H, H_{meta}, H_{para}, CH_{phenyl}); 8.14 (ddd, 2H, ^{4}J(H,H) = 2 Hz, ^{3}J(H,H) = 8 Hz, ^{3}J(P,H) = 15 Hz, H_{ortho}); 8.25 (d, 2H, ^{3}J(H,H) = 8 Hz, CH_{phenyl}) ; 9.50 (d, 2H, ^{3}J(H,H) = 8 Hz, CH_{phenyl}). ^{13}C NMR (100 MHz, $CDCl_3$): δ 12.0 (d, J (P,C) = 3 Hz, $PSCH_3$); 14.0 (s, CH_3); 14.1 (s, CH_3); 22.8 (s, CH_2); 25.8 (s, CH_2); 25.9 (s, CH_2); 28.9 (s, CH_2); 29,1 (s, CH_2); 31.5 (s, CH_2); 31.6 (s, CH_2); 68.7 (s, O CH_2); 69.7 (s, O CH_2); 97.4 (d, J(P,C) = 4 Hz , CH_{phenyl}); 102.4 (s, CH_{phenyl}); 111.6 (d, J(P,C)= 90 Hz, C□); 114.9 (d, J (P,C) = 60 Hz, C_{ipso}); 116.6 (d, J(P,C) = 10 Hz, C_{phenyl}); 122.0 (s, CH_{phenyl}); 122.8 (d, J(P,C)= 10Hz, C_{phenyl}); 129.0 (s, CH_{phenyl}); 131.4 (d, J(P,C)= 14 Hz, CH_{meta}); 131.8 (d, J(P,C)= 10 Hz, C_{phenyl}); 132.1 (s, C_{phenyl}); 132.4 (s, CH_{phenyl}); 132.5 (d, J(P,C)= 12 Hz, CH_{ortho}); 135.8 (d, J(P,C)= 2 Hz, C_{phenyl}); 136.8 (d, J(P,C) = 2 Hz, CH_{para}); 143.3 (d, J(P,C) = 18 Hz, Cβ); 160.2 (s, C_{phenyl}); 160.7 (d, J(P,C) = 3 Hz, C_{phenyl}). ^{31}P NMR (160 MHz, $CDCl_3$): δ +49.8 (s). HR MS (ESI, CH_2Cl_2/MeOH, 9/1, m/z): [M]+ calcd for $C_{59}H_{70}O_4PS$: 905.47325, Found 905.4723.

Compound **13b**. To a solution of 19 mg solution of compound **9b** in 10 mL of dichloromethane is added an excess of P(NMe2)3. The mixture immediately turned to yellow. Then, the solution is stirred during 30 min and filtered on basic alumina. Evaporation of solvents and washing with pentane under argon afford 12 mg of an orange powder (80%). 1H NMR (400 MHz, CDCl3): 0.95 (t, ^{3}J(H,H) = 6 Hz, 12H, CH_3); 1.20-1.65 (m, 24H, CH_2); 1.70-1.80 (m, 4H, CH_2); 2.00-2.10 (m, 4H, CH_2); 3.88- 4.22 (m, 8H, OCH_2); 6.65 (d, 2H, ^{4}J(H,H) = 2 Hz , CH_{phenyl}); 6.98 (m, 2H, CH_{phenyl}); 7.19 (ddd, 2H, ^{2}J(H,H) = 8 Hz, ^{2}J(H,H) = 8 Hz, ^{3}J(P,H) =1 Hz, H_{meta}); 7.28 (m, 1H, H_{para}); 7.51 (ddd, 2H, ^{2}J(P,H) = 8 Hz, ^{2}J(H,H) = 8 Hz, H_{ortho}); 7.73 (dd, 2H, ^{3}J(H,H) = 8 Hz, ^{3}J(H,H) = 8 Hz, CH_{phenyl}); 8.39 (d, 2H, ^{3}J(H,H) = 7Hz, CH_{phenyl}) ; 9.55 (d, 2H, ^{3}J(H,H) = 8.5 Hz, CH_{phenyl}). ^{13}C NMR (100 MHz, CD_2Cl_2): δ 14.1 (s, CH_3); 14.2 (s, CH_3); 22.6 (s, CH_2); 22.7 (s, CH_2); 25.8 (s, CH_2); 26.1 (s, CH_2); 29.1 (s, CH_2); 29,3 (s, CH_2); 31.6 (s, 2 CH_2); 67.9 (s, O CH_2); 69.1 (s, O CH_2); 100.0 (s, CH_{phenyl}); 100.1 (d, J(P,C) = 5 Hz, CH_{phenyl}); 114.9 (d, J(P,C) = 6 Hz , C_{phenyl}); 119.8 (s, CH_{phenyl}); 124.6 (s, C_{phenyl}); 127.4 (d, J(P,C) = 16 Hz, C_{phenyl}); 128.8 (d, J(P,C) = 9 Hz, CH_{meta}); 129.9 (s, C_{phenyl}); 131.7 (d, J(P,C) = 14 Hz, CH_{phenyl}); 134.4 (d, J(P,C) = 22 Hz, CH_{ortho}); 135.3 (d, J(P,C) = 14 Hz, CH_{para}); 136.8 (s, C6); 138.8 (d, J(P,C) = 6 Hz, Cβ); 158.0 (s, C_{phenyl}); 160.5 (d, J(P,C) = 3 Hz, C). Cipso, C1 and Cα are not observed. ^{31}P NMR (160 MHz, $CDCl_3$): δ -3.0 (s). HR

MS (ESI, CH_2Cl_2/MeOH, 9/1, m/z): [M+H]+ calcd for $C_{58}H_{68}O_4P$: 859.4855, Found 859.4851.

Compound **11b^O**. Compound **13b** (20 mg, 0.04 mmol, 1 eq.) was dissolved in 20 mL of dichloromethane. Excess of $NaIO_4$ was then added and the solution was stirred at RT for 2 h. Then the solvent were evaporated and the crude precipitate was purified by chromatography on silica gel using ethyl acetate as eluent to afford **11b^O** as an orange solid (70 %).^{1}H NMR (300 MHz, $CDCl_3$): δ 0.95 (t, 3J (H,H) = 6 Hz, 12H, CH_3); 1.39 (m, 16H, CH_2); 1.50 (m, 4H, CH_2); 1.58 (m, 4H, CH_2); 1.80 (m, 4H, CH_2); 1.98 (m, 4H, CH_2); 3.91-4.22 (m, 8H, O CH_2); 6.65 (d, 2H, ^4J(H,H) = 2 Hz, CH_{phenyl}); 7.15 (s, 2H, CH_{phenyl}); 7.28-7.35 (m, 2H, H_{meta}); 7.44 (m, 1H, H_{para}); 7.62 (dd, 2H, ^3J(H,H)= 8 Hz, ^{3}J(H,H) = 8 Hz, CH_{phenyl}); 7.93 (dd, 2H, ^3J(H,H) = 8 Hz, J(P,H) = 14 Hz, H_{ortho}); 8.13 (d, 2H, ^3J (H,H) = 8 Hz, CH); 9.38 (d, 2H, ^3J(H,H) = 8 Hz, CH). ^{13}C NMR (100 MHz, $CDCl_3$): δ 14.1 (s, CH_3); 14.2 (s, CH_3); 22.5 (s, CH_2); 22.6 (s, CH_2); 25.8 (s, CH_2); 26.0 (s, CH_2); 29.1 (s, CH_2); 29,2 (s, CH_2); 31.6 (s, CH_2); 31.7 (s, CH_2); 68.0 (s, O CH_2); 68.2 (s, O CH_2); 99.1 (d, J(P,C) = 5 Hz, C); 101.0 (s, CH_{phenyl}); 116.0 (d, J(P,C) = 6 Hz , C_{phenyl}); 120.6 (s, CH_{phenyl}); 123.3 (d, J(P,C) = 11 Hz, C); 124.6 (d, J(P,C) = 110 Hz, Cα); 128.1 (s, CHphenyl); 128.9 (d, J(P,C)= 13 Hz, CH_{meta}); 129.6 (s, CH_{phenyl}); 130.3 (d, J(P,C) = 100 Hz, C_{ipso}); 130.9 (d, J(P,C) = 12 Hz, CH_{ortho}); 132.1 (d, J(P,C) = 3 Hz, CH_{para}); 132.3 (d, J(P,C) = 4 Hz, C_{phenyl}); 133.4 (d, J(P,C) = 11 Hz, C); 134.0 (s, C_{phenyl}) ; 138.2 (d, J(P,C) = 20 Hz, Cβ); 158.8 (s, C_{phenyl}); 160.0 (d, J(P,C) = 2 Hz, C_{phenyl}). ^{31}P NMR (160 MHz, $CDCl_3$): δ +39.3 (s). HR MS (ESI, CH_2Cl_2/MeOH, 9/1, m/z): [M+H]+ calcd for $C_{58}H_{68}O_5P$: 875.4799, Found 875.4804.

Computational details. All calculations were carried out with the Gaussian 09 program package.[38] Full geometry optimization was performed for all molecules at the B3LYP/6-31+G* level[39,40] and subsequently harmonic vibrational frequencies were calculated at the same level to establish the nature of the stationary point obtained, for minima no negative eigenvalue of the Hessian was present. All possible rotational structures (based on methoxy rotations) have been investigated for **11a^S** (Table SX), the most stable one being that obtained also by X-ray crystallography (Figure S2). Molecular orbitals have been visualized with the VMD package.[41] TD DFT calculations were carried out at the B3LYP/6-31+G* level. Vertical excitation energies were obtained at the optimized geometries of the ground state. Vertical emission energies were obtained at the TD DFT geometry optimized geometries of the first excited states, which were always characterized as the HOMO-LUMO excited

electronic configuration. To estimate the effect of the solvent on the excitation energies, ionization energies and electron affinities, single point PCM calculations were carried out.

Adresses

*__Corresponding author__ : **Muriel Hissler**, Institut des Sciences Chimiques de Rennes, UMR6226 CNRS-Université de Rennes 1, Campus de Beaulieu, 35042 Rennes Cedex, France ; E-mail: mhissler@univ-rennes1.fr; **László Nyulászi**, Department of Inorganic and Analytical Chemistry, Budapest University of Technology and Economics, Szt. Gellért tér 4, Budapest 1111, Hungary; E-mail: nyulaszi@mail.bme.hu

Rózsa Szűcs, François Riobé, Aude Escande, Damien Joly and Pierre-Antoine Bouit : Institut des Sciences Chimiques de Rennes, UMR6226 CNRS-Université de Rennes 1, Campus de Beaulieu, 35042 Rennes Cedex, France

Rózsa Szűcs : Department of Inorganic and Analytical Chemistry, Budapest University of Technology and Economics, Szt. Gellért tér 4, Budapest 1111, Hungary

Supplementary Materials

NMR data, spectroscopic tables and computational details are available in the supplementary materials.

References

[1] M. D. Watson, A. Fechtenkötter, K. Müllen, *Chem. Rev.* **101**, 1267 (2001).

[2] J. Wu, W. Pisula, K. Müllen, K. *Chem. Rev.* **107**, 718 (2007).

[3] L. Schmidt-Mende, A. Fechtenkötter, K. Müllen, E. H. Moons, R. Friend, J. D. MacKenzie, J. D *Science* **293**, 1119 (2001).

[4] S. M. Draper, D. J. Gregg, R. Madathil, *J. Am. Chem. Soc.* **124**, 3486 (2002).

[5] D. Wu, W. Pisula, M. C. Haberecht, X. Feng, K. Müllen, *Org. Lett.* **11**, 5686 (2009).

[6] N. K. S. Davis, A. L. Thompson, H. L. Anderson, *J. Am. Chem. Soc.* **133**, 30 (2011).

[7] C. Dou, S. Saito, K. Matsuo, I. Hisaki, S. Yamaguchi, *Angew. Chem. Int. Ed.* **51**, 12206 (2012).

[8] M. Stępień, E. Gońka, M. Żyła, N. Sprutta, *Chem. Rev.* **2016**, 10.1021/acs.chemrev.6b00076.

[9] P. O. Dral, M. Kivala, T. J. Clark, *J. Org. Chem.* **78**, 1894 (2013).

[10] L. Nyulászi *Chem. Rev.* **101**, 1229 (2001).

[11] T. Hatakeyama, S. Hashimoto, M. Nakamura, *Org. Lett.* ***13***, 2130 (2011).

[12] L. Chen, Y. Hernandez, X. Feng, K. Müllen, *Angew. Chem. Int. Ed.* 51, 7640 (2012).

[13] M. Grybowski, K. Skonieczny, H. Butenschön, D. T. Gryko, *Angew. Chem. Int. Ed.* **52**, 9900 (2013).

[14] A. Narita, X. Feng, Y. Hernandez, S. A. Jensen, M. Bonn, H. Yang, I. A. Verzhbitskiy, C. Casiraghi, M. R. Hansen, A. H. R. Koch, G. Fytas, O. Ivasenko, B. Li, K. S. Mali, T. Balandina, S. Mahesh, S. De Feyter, K. Müllen, *Nat. Chem.* **6**, 126 (2014).

[15] L. Chen, S. R. Puniredd, Y.-Z. Tan, M. Baumgarten, U. Zschieschang, V. Enkelmann, W. Pisula, X. Feng, H. Klauk and K. Müllen, *J. Am. Chem. Soc.* **134**, 17869 (2012).

[16] A. A. Gorodetsky, C.-Y. Chiu, T. Schiros, M. Palma, M. Cox, Z. Jia, W. Sattler, I. Kymissis, M. Steigerwald and C. Nuckolls, *Angew. Chem. Int. Ed.* **49**, 7909 (2010).

[17] P.-A. Bouit, A. Escande, R. Szűcs, D. Szieberth, C. Lescop, L. Nyulászi, M. Hissler, R. Réau, *J. Am. Chem. Soc.* **134**, 6524 (2012).

[18] F. Riobé, R. Szűcs, P.-A. Bouit, D. Tondelier, B. Geffroy, F. Aparicio, J. Buendía, L. Sánchez, R. Réau, L. Nyulászi, M. Hissler, *Chem. Eur. J.* **21**, 6547 (2015).

[19] L. Zhai, R. Shukla, R. Rathore, *Org. Lett.***11**, 3474 (2009).

[20] V. K. Reedy, L. N. Rao, M. Maeda, B. Haritha, M. Yamashita, *Heteroatom Chemistry* **14**, 320 (2003).

[21] L. Nyulaszi, O. Holloczki, C. Lescop, M. Hissler, R. Réau, *Org. Biomol. Chem.* **4**, 996 (2006).

[22] O. Fadhel, D. Szieberth, V. Deborde, C. Lescop, L. Nyulászi, M. Hissler, R. Réau, *Chem. Eur. J.* **15**, 4914 (2009).

[23] L. Liu, B. Yang, T. J. Katz, M. K. Poindexter, *J. Org. Chem.* **56**, 3769 (1991).

[24] W. Delaunay, R. Szűcs, S. Pascal, A. Mocanu, P. A. Bouit, L. Nyulaszi, M. Hissler, *Dalton Trans.* **45**, 1896 (2016).

[25] S. H. Wadumethrige, R. Rathore, *Org. Lett.* **10**, 5139 (2008).

[26] Y. Matano, T. Miyajima, T. Fukushima, H. Kaji, Y. Kimura, H. Imahori, *Chem. Eur. J.* **14**, 8102 (2008).

[27] P. von Raqué Schleyer, C. Maerker, A. Dransfeld, H. Jiao N. J. R. van Eikema Hommes, *J. Am. Chem. Soc.* **118**, 6317 (1996).

[28] P. von Ragué Schleyer, H. Jiao, N. J. R. van Eikema Hommes, V. G. Malkin, O. L. Malkina, *J. Am. Chem. Soc.* **119**, 12669 (1997).

[29] P. von Ragué Schleyer, M. Manoharan, Z. X. Wang, B. Kiran, H. Jiao, R. Puchta, N. J. R. van Eikema Hommes, *Org. Lett.* **3**, 2465 (2001).

[30] C. W. Bird, *Tetrahedron* **41**, 1409 (1985)

[31] L. Nyulászi, P. Várnai, T. Veszprémi, *Journal of Molecular Structure: THEOCHEM* **358**, 55 (1995).

[32] Benkő, Z.; Nyulászi, L. *Aromatic Phosphorus Heterocycles. In Aromaticity in Heterocyclic Compounds. T. M. Krygowski, M. KCyransky, (Editors). Vol 19 in Topics in Heterocyclic Chemistry* (Gupta R. R. (Series Editor) Springer, Heidelberg, 27-83 (2009).

[33] Szucs, R.; Bouit, P. -A.; Hissler, M.; Nyulaszi, L. *Struct.Chem.* **26**, 1351 (2015).

[34] D. Joly, P. -A. Bouit, M. Hissler, *J. Mater. Chem. C* **4**, 3686 (2016).

[35] M. Duffy, W. Delaunay, P.-A. Bouit, M. Hissler, *Chem. Soc. Rev*. **45**, 5296 (2016).

[36] M. J. Mio, L. C. Kopel, J. B. Braun, T. L. Gadzikwa, K. L. Hull, R. G. Brisbois, C. J. Markworth, P. A. Grieco *Org. Lett.* **4**, 3199 (2002).

[37] A. L. Stein, J. da Rocha, P. H. Menezes, G. Zeni, *Eur J. Org.Chem.* **4**, 705 (2010).

[38] Gaussian 09, Revision B.01, M. J. Frisch, G. W. Trucks, H. B. Schlegel, G. E. Scuseria, M. A. Robb, J. R. Cheeseman, G. Scalmani, V. Barone, B. Mennucci, G. A. Petersson, H. Nakatsuji, M. Caricato, X. Li, H. P. Hratchian, A. F. Izmaylov, J. Bloino, G. Zheng, J. L. Sonnenberg, M. Hada, M. Ehara, K. Toyota, R. Fukuda, J. Hasegawa, M. Ishida, T. Nakajima, Y. Honda, O. Kitao, H. Nakai, T. Vreven, J. A. Montgomery, Jr., J. E. Peralta, F. Ogliaro, M. Bearpark, J. J. Heyd, E. Brothers, K. N. Kudin, V. N. Staroverov, T. Keith, R. Kobayashi, J. Normand, K. Raghavachari, A. Rendell, J. C. Burant, S. S. Iyengar, J. Tomasi, M. Cossi, N. Rega, J. M. Millam, M. Klene, J. E. Knox, J. B. Cross, V. Bakken, C. Adamo, J. Jaramillo, R. Gomperts, R. E. Stratmann, O. Yazyev, A. J. Austin, R. Cammi, C. Pomelli, J. W. Ochterski, R. L. Martin, K. Morokuma, V. G. Zakrzewski, G. A. Voth, P. Salvador, J. J. Dannenberg, S. Dapprich, A. D. Daniels, O. Farkas, J. B. Foresman, J. V. Ortiz, J. Cioslowski, D. J. Fox, Gaussian, Inc., Wallingford CT, 2010.

[39] A. D. Becke *J. Chem. Phys*. **98**, 5648 (1993).

[40] C. Lee, W. Yang, R. G. Parr. *Phys. Rev. B* **37**, 785 (1988).

[41] Humphrey, W., Dalke, A. Schulten, K., "VMD - Visual Molecular Dynamics", *J. Molec. Graphics* **14**, 33 (1996).